

Matching of a Multimodule Plasma Opening Switch to a Liner Load

G. I. Dolgachev, D. D. Maslennikov, A. G. Ushakov, A. S. Fedotkin, and I. A. Khodeev

Russian Research Centre Kurchatov Institute, pl. Kurchatova 1, Moscow, 123182 Russia

Received January 25, 2007; in final form, March 22, 2007

Abstract—One of the key problems of the Baikal project, intended to create a superpower pulsed generator for ICF experiments, is that of matching a multimodule plasma opening switch (POS) to a liner load. An intermediate inductance or a separating discharger is proposed to be used as a matching element between the POS and the load. An analysis is made of the effect of both versions of the matching system on the synchronization of the POS modules and the energy transfer from the inductive storage to the load. Methods for optimizing the matching element are examined. It is shown that the POS modules can be synchronized and the inductive storage energy can be efficiently transferred to a low-impedance load. A multigap vacuum discharger with a point anode and plane cathode is to be used as a separating discharger. Such an electrode system make it possible to concentrate the electric field at the point anode and to substantially enhance the electric strength of the inter-electrode gap. Results are presented from experimental studies of vacuum breakdown in such an electrode system with a gap length of about 1 mm.

PACS numbers: 52.59.Mv, 52.75.Kq, 84.70.+p

DOI: 10.1134/S1063780X07100042

1. INTRODUCTION

In the Baikal program, intended to create a superpower pulsed generator for ICF experiments, a plasma opening switch (POS) is planned to be used as an output power sharpener [1]. To increase the commutated current and output voltage, it is proposed to use a multimodule erosion POS with an external magnetic field produced by an independent source [2]. The use of a liner as a load at the output of the multimodule POS implies that such a POS should be matched to the load. The low initial impedance of the liner leads to the short-circuiting of the POS, because even a slight increase in the POS resistance is accompanied by the switching of the current to the load. The result is that, because of the redistribution of the current between the POS modules, the process of their synchronization terminates, no energy goes into ion acceleration (i.e., into plasma erosion), and the POS becomes closed again, thereby disconnecting the load from the inductive energy storage.

An analysis of the experimental data [3] on the synchronization of two parallel modules, each connected to its own load (Fig. 1), shows that the scatter in the operation times of the POS modules (see Fig. 2) is

$$\Delta t \sim Z_c/Z_l, \quad (1)$$

where Z_c is the impedance of the coupling circuit between the modules and Z_l is the load impedance. The low initial liner impedance $Z_l \approx 0$ makes the synchronization of the modules impossible, because, according to formula (1), the scatter in their operation times is then very large.

For the same reason, the energy from the inductive storage cannot be transferred to the liner: even at a very low voltage at the POS, the current is switched to the liner, whose initial impedance is nearly zero. After this, no energy is deposited in the POS and, therefore, the process of plasma erosion and creation of a magnetically insulated vacuum gap between the POS electrodes terminates. As a result, the POS recloses, thereby shutting off the inductive energy storage from the load and preventing energy transfer to the imploding liner. The

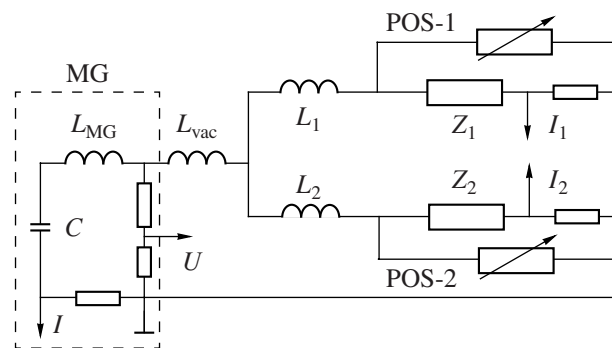


Fig. 1. Electric circuit of the experiment on the synchronization of POS-1 and POS-2 in the A-2S facility [2] with a Marx generator (MG) ($C = 7 \times 10^{-2} \mu\text{F}$, $U = 1 \text{ MV}$) and storage inductance ($L_0 = L_{\text{MG}} + L_{\text{vac}} = 17 \mu\text{H}$). Here, L_1 and L_2 are the inductances of the connection circuit ($L_1 = L_2 = 1 \mu\text{H}$), Z_1 and Z_2 are the load impedances, and I_1 and I_2 are the load currents.

aim of the present work is to eliminate the effect of a low-impedance load on the POS operation and to create conditions for the synchronization of the modules and efficient transfer of the inductive storage energy to the liner load, whose impedance is initially low and increases with time. For this purpose, we propose to install a matching element between the POS and the load (Fig. 3).

2. INDUCTANCE AS A MATCHING ELEMENT OF THE POS-LINER SYSTEM

One possible way of reducing the effect of a low-impedance load on the POS operation (i.e., of matching a multimodule POS to the liner load) is to use an intermediate inductance L_{int} between the POS and the load. If we assume that the liner impedance remains low during the POS operation, then the intermediate inductance will act as a load and the total energy stored in it will be released in the liner, regardless of whether the POS is reclosed or not. This assumption is quite realistic, because, in the liner acceleration experiments carried out in the Stend-300 [4], Angara-5 [5], and PBFA [6] facilities at load currents of 2–20 MA and current rise times of 60–120 ns, the liner began to accelerate and, accordingly, the energy began to be absorbed in it when the current approached its maximum. Of course, such behavior of the liner over a wide range of the load currents is not accidental but is a consequence of the optimization of the liner mass.

Taking account the above assumption, we can estimate the current in the intermediate inductance I_{int} , the energies remaining in the intermediate and storage inductances (W_{int} and $W_{0 \text{ rem}}$, respectively), the efficiency of energy transfer to the intermediate inductance η , and the energy W_{POS} released in the POS:

$$I_{\text{int}} = I_0 L_0 / (L_0 + L_{\text{int}}), \quad (2)$$

$$W_{\text{int}} = W_0 \eta = W_0 L_0 L_{\text{int}} / (L_0 + L_{\text{int}})^2, \quad (3)$$

$$W_{0 \text{ rem}} = W_0 [L_0 / (L_0 + L_{\text{int}})]^2, \quad (4)$$

$$\begin{aligned} W_{\text{POS}} &= W_0 - (W_{\text{int}} + W_{0 \text{ rem}}) \\ &= W_0 (L_0 L_{\text{int}} + L_{\text{int}}^2) / (L_0 + L_{\text{int}})^2, \end{aligned} \quad (5)$$

where I_0 and W_0 are the current and energy in the storage inductance L_0 by the beginning of POS operation and η is the efficiency of energy transfer to the intermediate inductance. Note that, when the POS is reclosed by plasma, the intermediate inductance L_{int} is disconnected from the storage inductance L_0 . As a result, only the energy transferred to the inductance L_{int} is released in the imploding liner; i.e., the efficiency of energy transfer to the liner is determined by the same quantity η . If the POS is not reclosed by plasma (this can occur only with a high-impedance load, i.e., when $L_{\text{int}}/L_0 \geq 1$), then both the energy transferred to the intermediate inductance L_{int} and the energy remaining in the storage

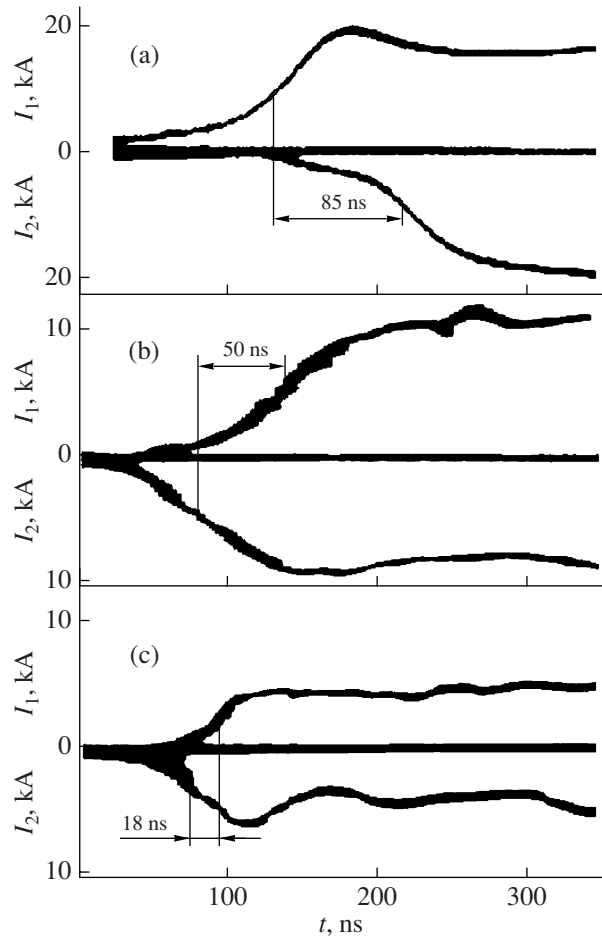


Fig. 2. Typical waveforms of the currents in the POS-1 and POS-2 loads at different ratios of the coupling inductance impedance Z_c to the load impedance $Z_{1,2}$: (a) $Z_c/Z_{1,2} = 1$ ($Z_{1,2} = 15 \Omega$), (b) $Z_c/Z_{1,2} \approx 0.04$ ($Z_{1,2} \approx 400 \Omega$), and (c) $Z_c/Z_{1,2} \approx 0.02$ ($Z_{1,2} \approx 800 \Omega$).

inductance L_0 can be released in the imploding liner. In this case, the efficiency of energy transfer to the liner reaches its maximum possible value η_{max} :

$$\eta_{\text{max}} = (W_{\text{int}} + W_{0 \text{ rem}}) / W_0 = L_0 / (L_0 + L_{\text{int}}), \quad (6)$$

which coincides with I_{int}/I_0 in formula (2). The actual efficiency of energy transfer to the liner lies in the range $\{\eta, \eta_{\text{max}}\}$.

Formula (5) allows us to estimate the POS voltage, which, according to [7], is a function of the energy density w (or the total energy W_{POS}) expended on the acceleration of ions (i.e., on plasma erosion):

$$U_{\text{POS}} \propto w^{4/7} \propto W_{\text{POS}}^{4/7}. \quad (7)$$

In the absence of a load, the total energy of the inductive storage is released in the POS (i.e., $W_{\text{POS}} = W_0$) and,

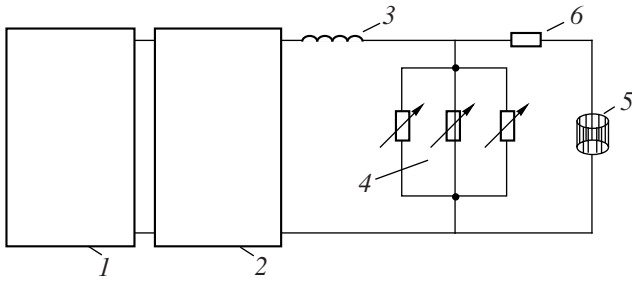


Fig. 3. Electric circuit of the matching element connection in high-power generators with parallel-connected POS modules: (1) primary energy source, (2) stages of intermediate pulse sharpening, (3) inductive energy storage, (4) multimodule POS, (5) load (liner), and (6) matching element in the “POS modules–load” circuit.

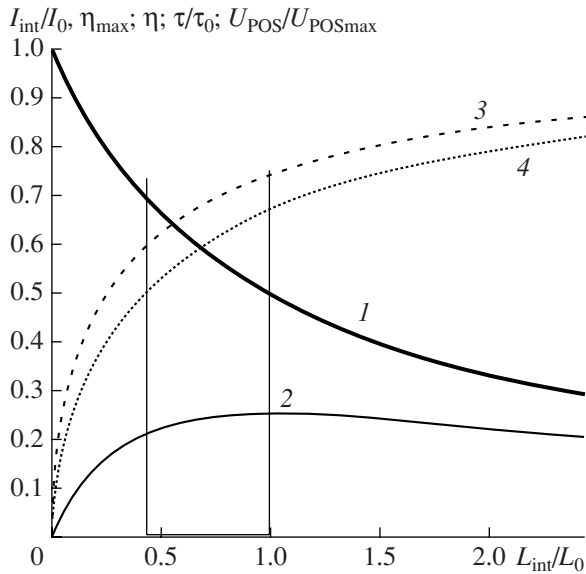


Fig. 4. Parameters of the energy pulse transferred to the load as functions of the normalized intermediate (matching) inductance L_{int}/L_0 : (1) normalized current flowing through the intermediate inductance, I_{int}/I_0 (formula (2)), and the maximum efficiency of energy transfer to the load (liner), η_{max} , without POS reclosure (formula (6)); (2) efficiency of energy transfer to the intermediate inductance (and the liner), $\eta = W_{\text{int}}/W_0$, in the case of POS reclosure (formula (3)); (3) relative duration of the current front in the intermediate inductance, τ/τ_0 (formulas (10) and (11)); and (4) normalized POS voltage $U_{\text{POS}}/U_{\text{POSmax}}$ (formula (9)).

according to formula (7), the POS voltage reaches its maximum value

$$U_{\text{POSmax}} = \alpha_{1,2} U_{\text{MG}}^{4/7}, \quad (8)$$

where the POS voltage U_{POSmax} and the voltage U_{MG} of the primary storage (Marx generator) are expressed in megavolts and the factor $\alpha_1 = 2.5(\text{MV})^{-3/7}$ for a POS without a magnetic field and $\alpha_2 = 3.6(\text{MV})^{-3/7}$ for a

POS with an external magnetic field. Formulas (5), (7), and (8) allow us to estimate the POS voltage U_{POS} in the presence of an inductive load L_{int} ,

$$U_{\text{POS}} = U_{\text{POSmax}} (W_{\text{POS}}/W_0)^{4/7} \quad (9)$$

$$= U_{\text{POSmax}} [(L_0 L_{\text{int}} + L_{\text{int}}^2)/(L_0 + L_{\text{int}})^2]^{4/7}.$$

The voltage pulse duration (i.e., the duration of the leading edge of the current pulse switched into the intermediate inductance) can be estimated as

$$\tau \approx L_{\text{int}} I_{\text{int}} / U_{\text{POS}}. \quad (10)$$

It should be noted that, in the absence of a load (this corresponds to $L_{\text{int}} \rightarrow \infty$), the measured value τ_0 of the voltage pulse duration is 100–150 ns, i.e.,

$$\tau_0 \approx L_0 I_0 / U_{\text{POSmax}} \approx 100\text{--}150 \text{ ns}. \quad (11)$$

Figure 4 shows the amplitude of the current pulse in the intermediate inductance (load) I_{int} , the duration of its leading edge τ , the efficiency of energy transfer to the intermediate inductance (or the liner) η , the maximum efficiency of energy transfer to the liner η_{max} , and the voltage U_{POS} , calculated by formulas (2), (3), (6), (9), (10), and (11) as functions of the intermediate inductance L_{int} .

These dependences illustrate the main constraint of the inductive energy storage: it is impossible to simultaneously achieve high load currents and high load voltages. High voltages can be achieved only by reducing the load current. Thus, in the MOL facility [1, 8], the value of the connecting inductance in the POS–liner circuit (which simultaneously acts as an intermediate inductance L_{int}) can be reduced to $\sim 0.1L_0$; as a result, the current switched to the liner may be increased to $\sim 0.9I_0$. However, in this case, the efficiency of energy transfer to the liner will be $\sim 5\%$ and the voltage will not exceed $0.2U_{\text{POSmax}}$.

At the same time, it can be seen from Fig. 4 that, when the intermediate inductance is in the range $L_{\text{int}}/L_0 = 0.4\text{--}1$, the parameters of the current pulse switched to L_{int} (and, accordingly, to the liner) can be quite acceptable:

$$\eta = 0.2\text{--}0.25, \quad \eta_{\text{max}} = 0.5\text{--}0.7,$$

$$U_{\text{POS}} = (0.45\text{--}0.68)U_{\text{POSmax}}, \quad I_{\text{int}} = (0.5\text{--}0.7)I_0,$$

$$\tau = (0.55\text{--}0.7)\tau_0 \approx 55\text{--}100 \text{ ns}.$$

At these parameters, the POS modules can be synchronized with an accuracy of $\Delta t = 20\text{--}50$ ns. In this case, $\Delta t \approx 20$ ns corresponds to $L_{\text{int}}/L_0 = 1$ and $\Delta t \approx 50$ ns, to $L_{\text{int}}/L_0 = 0.4$. To ensure such an accuracy, it is necessary that the condition $Z_c/Z_l = L_c/L_{\text{int}} \leq 0.04$ be satisfied (see Fig. 2), which can easily be achieved in practice. Indeed, the coupling inductance between the modules is $L_c \approx 0.05L_{\text{int}}$, where $L_{\text{int}} = (0.45\text{--}1)L_0$, which allows the above condition $L_c/L_{\text{int}} = 0.02\text{--}0.05$ to be easily satisfied. At a synchronization accuracy of 20–50 ns, the

duration of leading edge of the current pulse will increase to $(55 + 50) - (100 + 20) \text{ ns} = 100\text{--}120 \text{ ns}$. This estimate of the current rise time falls within the range of current fronts in liner experiments. The plots in Fig. 4 allow us to optimize the ratio L_{int}/L_0 by taking the optimal (for the liner acceleration) combination of the values of η , η_{max} , U_{POS} , I_{int} , and τ .

Hence, the use of an intermediate inductance as a matching element allows one to eliminate the effect of the liner (a load with a nearly zero initial impedance) on the POS operation, because, in this case, the POS is loaded with the high-impedance load L_{int} . Moreover, the use of an intermediate inductance as an energy source for liner acceleration eliminates restrictions imposed on the POS voltage, which is actually limited by a value of $\sim 5 \text{ MV}$. In this case, the voltage is generated by the intermediate inductance itself and is determined by the liner dynamics. Therefore, in the Baikal project, it is possible to abandon the idea of the use of two oppositely connected POSs for generating a voltage of $\sim 10 \text{ MV}$.

3. MATCHING OF THE POS-LINER SYSTEM BY USING A SEPARATING DISCHARGER

The second method for matching a multimodule POS to the liner load is to install a separating discharger between the load and the common output of the POS modules. This allows one to achieve good synchronization of the modules and optimum energy transfer to the load. Before gap breakdown, we have $Z_l \rightarrow \infty$. In this case, according to formula (1), the POS modules are rapidly synchronized, the difference between the operation times of the modules being $\Delta t \sim Z_c/Z_l \approx 0$. In fact, in experiments on the synchronization of the POS modules [9], the use of a separating discharger made it possible to redistribute the currents between the modules, to achieve the high resistance of each module, and to switch the current to a low-inductance load after the breakdown of the discharger. In this case, the POS modules operate as a single POS with the summary number of plasma guns. Moreover, with the use of a separating discharger, the energy released in the POS is high enough to achieve deep plasma erosion and the high resistance and high electric strength of the POS interelectrode gap. As a result, the energy that remains in the inductive energy storage by the instant of breakdown can be expended on the acceleration the liner, even if its initial impedance is low.

Using formulas (7) and (8), we can estimate the POS output voltage as a function of the energy transferred to the load or as a function of the load impedance Z_l ,

$$U_{\text{POS}} = U_{\text{POSmax}}(1 - \eta)^{4/7}. \quad (12)$$

Taking into account that

$$\eta = Z_l/(Z_{\text{POS}} + Z_l), \quad (13)$$

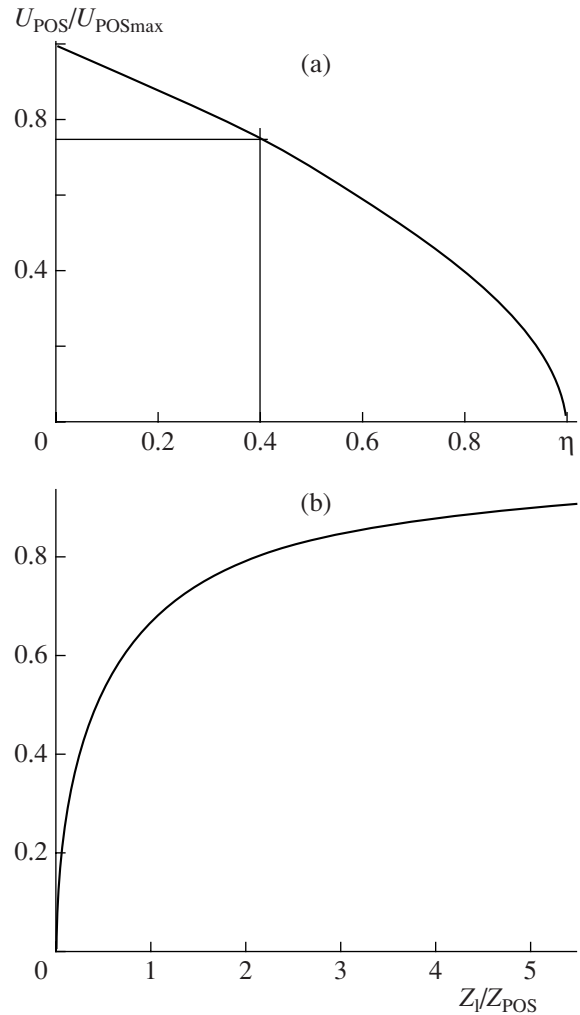


Fig. 5. Normalized voltage $U_{\text{POS}}/U_{\text{POSmax}}$ as a function of (a) the efficiency of energy transfer to the load, $\eta = W_l/W_0$, and (b) the normalized load impedance Z_l/Z_{POS} .

we obtain

$$U_{\text{POS}} = U_{\text{POSmax}}[(Z_l/Z_{\text{POS}})/(1 + Z_l/Z_{\text{POS}})]^{4/7}. \quad (14)$$

Figures 5a and 5b show the POS voltage as a function of the efficiency of energy transfer to the load and of the load impedance, respectively. The use of a separating discharger allows one to control both the energy released in the POS and the POS voltage. Thus, if the breakdown voltage of the separating discharger is $0.8U_{\text{POSmax}}$ (see Fig. 5a), then 40% of the inductive storage energy can be transferred to the liner load, i.e., to the load whose impedance is initially low and increases with time. Of course, this is an upper estimate of the energy that can be transferred to the load. Actually, the transferred energy is determined by the ratio of the rate with which the POS is closed by plasma to the growth rate of the load impedance. In experiments with a capacitive load (an analog of a liner [8]), the use of a separating discharger made it possible to transfer $\sim 25\%$

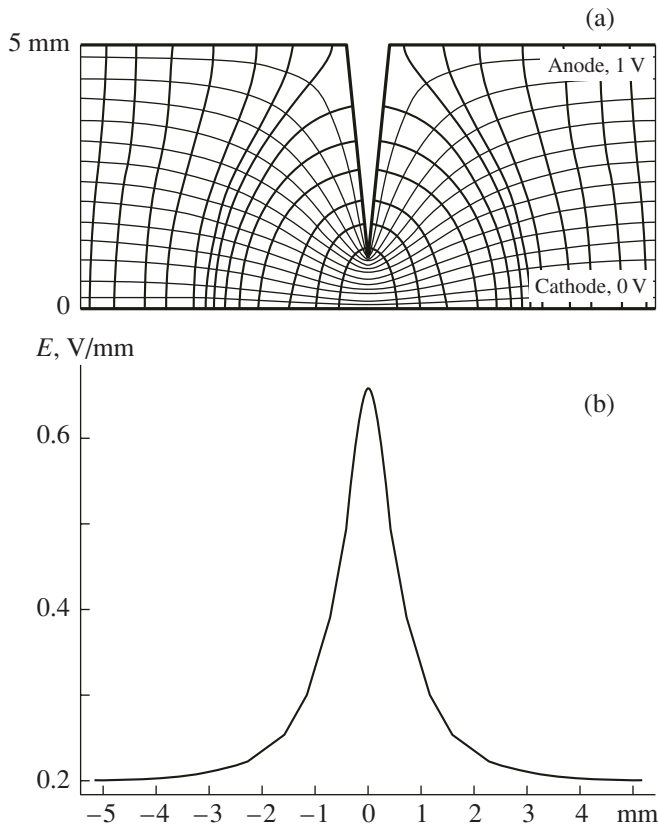


Fig. 6. Geometry of the point–plane electrode system and distribution of the electric field at a gap voltage of 1 V: (a) electric field lines and contour lines of the electric potential in the interelectrode space and (b) distribution of the normal component of the electric field over the cathode surface.

of the inductive storage energy to the load and to avoid the POS reclosure during $\sim 1 \mu\text{s}$. Hence, the separating discharger is a good matching element, which allows one not only to synchronize the POS modules but also to efficiently transfer energy to the liner.

4. DESIGN AND OPERATION OF THE SEPARATING DISCHARGER

In [10], a vacuum multigap explosive-emission diode [11] was proposed for the use as a separating discharger. The electric strength of such a discharger is determined by the total electric strength of all the gaps, and the operating time is equal to the closure time of one gap ($\sim 1 \text{ mm}$), because all the gaps are closed simultaneously.

In the microsecond range, breakdown of a millimeter gap can occur when the electric field strength exceeds the threshold value for explosive emission ($E \geq 100 \text{ kV/cm}$), i.e., at voltages of $U > 10 \text{ kV}$. A discharger of this type was used in [9]. In a superpower generator operating at a voltage of $\geq 3 \text{ MV}$, it is necessary to use ~ 50 gaps, which is rather difficult from the technological standpoint. To enhance the electric strength of a mil-

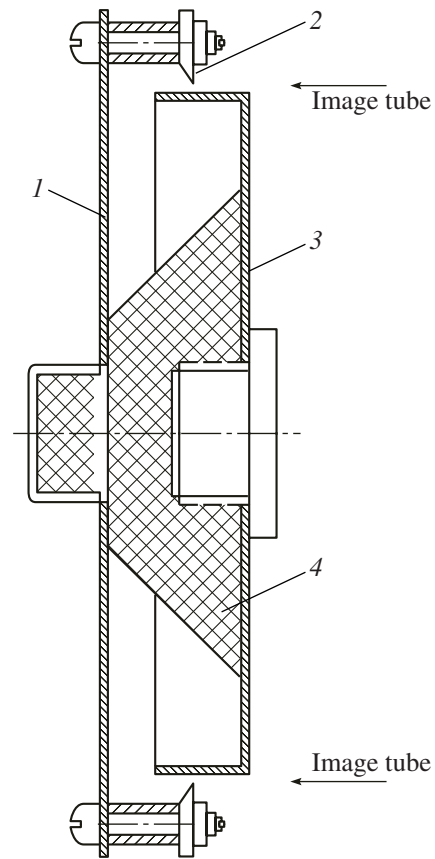


Fig. 7. Schematic of the annular discharger: (1) anode fastener, (2) annular anode edge, (3) cathode, and (4) insulator.

limeter gap (in other words, to reduce the number of discharge gaps), an electrode system with a plane cathode and an anode in the form of a sharp edge was proposed in [12]. Such a gap geometry allows one to concentrate the electric field at the sharp edge of the anode and, accordingly, to enhance the electric strength of the gap (Fig. 6). Calculations of the electric field for different electrode geometries show that variations in the edge sharpening angle in the range $15^\circ\text{--}30^\circ$ and the edge thickness in the range $0.05\text{--}3 \text{ mm}$ only slightly affect the electric field strength at the plane cathode. The electric field distribution presented in Fig. 6b demonstrates that, for the threshold electric field for explosive emission ($E \geq 100 \text{ kV/cm}$) to be achieved at the cathode surface in this electrode geometry, the applied voltage should be higher by a factor of 1.5 than that in a system with plane electrodes, i.e., the electric strength of the gap should increase by one-half.

Experimental studies of the dependence of the voltage pulse duration on the voltage amplitude [12] showed that the increase in the electric strength of a millimeter gap between the plane and the sharp edge is, in fact, much greater than it follows from the calculated field distribution. We performed two series of experi-

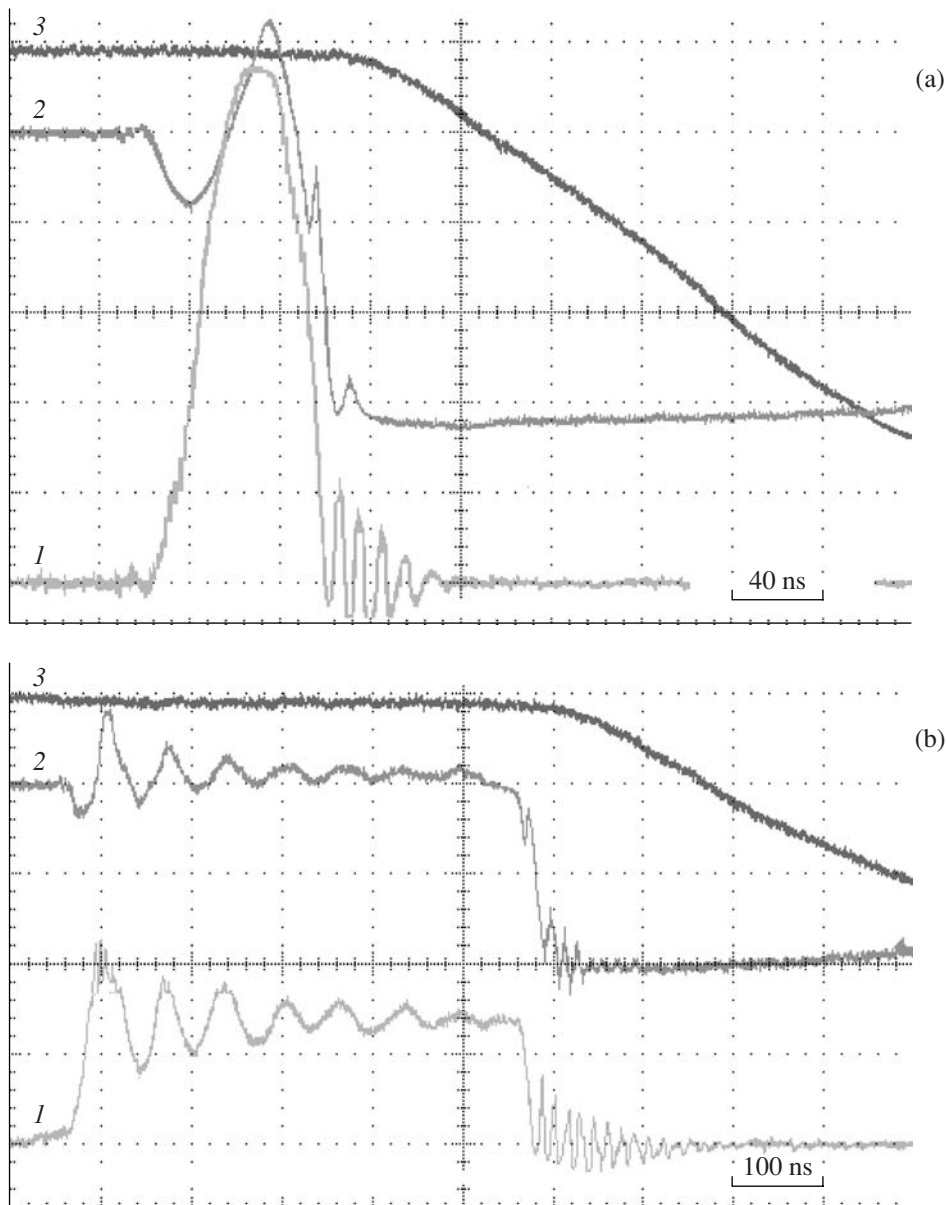


Fig. 8. Oscillograms of the annular discharger parameters for an MG voltage of (a) 110 and (b) 50 kV: (1) voltage (25 kV/div), (2) loop signal (20 kV/div or 8×10^9 (A/s)/div), and (3) current (12.5 kA/div).

ments: (i) with a short (4 mm) anode edge, which allowed the electrode plasma to be observed in two directions, and (ii) with a model single-gap discharger with a 160-mm-diameter annular anode edge (Fig. 7). In both cases, the sharpening angle of the anode edge was 15° (the edge easily cut paper). As a pulsed voltage source, we used a three-stage MG, which provided the current and charge densities as high as ~ 10 kA/cm and ~ 2 mC/cm, respectively. This roughly corresponds to the parameters of the MOL facility [13] (~ 10 kA/cm and 1 mC/cm, the diameter of the anode annular edge being ~ 1 m).

Typical oscillograms of the gap voltage, current time derivative, and discharge current (measured with a voltage divider, wire loop, and current shunt, respectively) are shown in Fig. 8. It can be seen that the duration of breakdown (i.e., the duration of the active electron-beam stage) is ~ 25 ns. This is the time interval from the beginning of breakdown to the instant at which the gap is bridged by streamers and the current begins to flow through it. Over most of this period, the current through the gap is close to zero. The actual duration of the transition from the high-resistance stage to the stage of the current growth and short-circuiting of the gap is about 10 ns. It is the duration of the transition

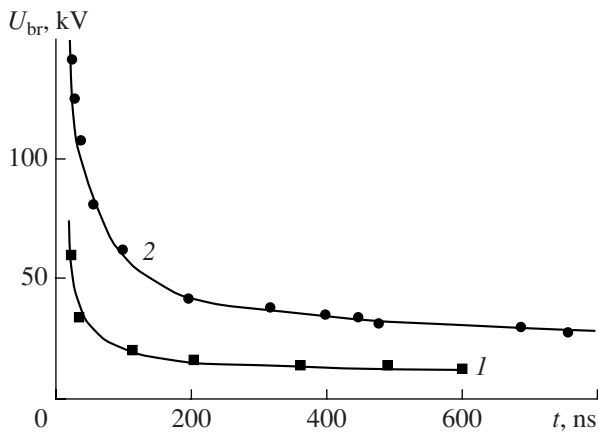


Fig. 9. Breakdown voltage U_{br} for different 1-mm gaps: (1) plane-electrode gap [10] and (2) disk gap with a sharp anode edge.

stage from a nonconducting to a conducting state that is referred to as the breakdown time. These oscillograms allow one to estimate the energy released in the gap during breakdown. The energy released per unit length of the anode edge is about 0.1 J/cm and depends only slightly on the voltage amplitude, because the duration of the active phase decreases with increasing voltage. The dependence of the voltage pulse duration on the voltage amplitude (see Fig. 9) has the same shape as that in the case of plane electrodes [10]. The electric strength of a “sharp edge–plane” gap increases by a factor of 3 as compared to a “plane–plane” gap, rather than by a factor of 1.6 as would be expected from the calculated distribution of the electric field. Such a significant enhancement of the electric strength of the gap is explained by the dynamics of the anode plasma (see Fig. 10). In the gap photographs taken with an image tube in the case of a short anode edge, it can be seen that

the side surfaces of the sharp edge undergo electron bombardment. One can trace the radial dynamics of the anode plasma glow, which expands in the direction perpendicular to the side surfaces of the anode edge, i.e., at an angle to the cathode plane. As a result, at the same field strength at the cathode, i.e., at a higher voltage at the anode edge, the voltage pulse duration is longer than that in the case of a plane anode. This means that, if we want to obtain pulses of equal duration, we must even further increase the voltage at the edge anode. Thus, at the same pulse duration, the electric strength of a gap with an edge anode is somewhat higher than that corresponding to the threshold electric field at the cathode (which is the same, $E \geq 100$ kV/cm, for both the edge and plane anodes). Tracks from electron bombardment of the anode surface can be seen in photographs taken with an image tube (see Fig. 10).

Figure 11 shows photographs of the gap glow in a model annular anode with a sharp edge. A comparison of the photographs taken with an image tube at different voltages (cf. Figs. 11b, 11c and Figs. 11d, 11e) shows that the number of breakdown channels increases with voltage. This is because an increase in the voltage is accompanied by an increase in the number of micropoints at which the conditions for explosive emission are satisfied: the cold-emission current from the highest micropoints is too low to cause a decrease in the gap voltage. Therefore, cold emission also occurs from the lower micropoints the current through which is zero at a lower voltage. A comparison of the image-tube photographs (Figs. 11a, 11b, 11d) and the integral photographs (Figs. 11c, 11e) taken at the same voltage show that the number of breakdown channels remains unchanged (i.e., no new micropoints come into play) throughout the current pulse. As the current flows through the gap, the individual channels broaden, but their total number remains the same. Due to the large area of the bombarded surface and the low energy den-

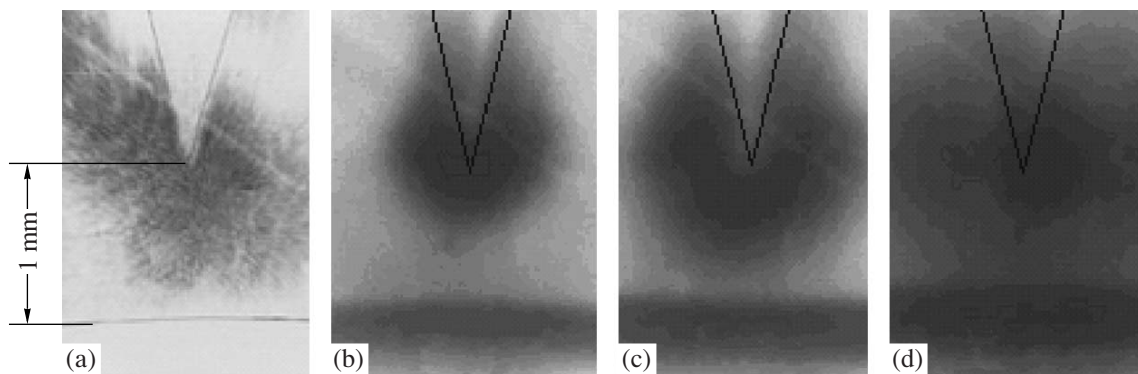


Fig. 10. Time evolution of the gap glow (the edge view): (a) photograph of the electrodes, taken in the laser light, and (b–d) photographs of the gap glow taken with an image tube (with an exposure of ~50 ns) at different delay times t_{del} with respect to the gap breakdown, $t_{del} =$ (b) 50, (c) 100, and (d) 200 ns. The MG voltage is 87–90 kV. The electrode contours are displayed with heavy lines.

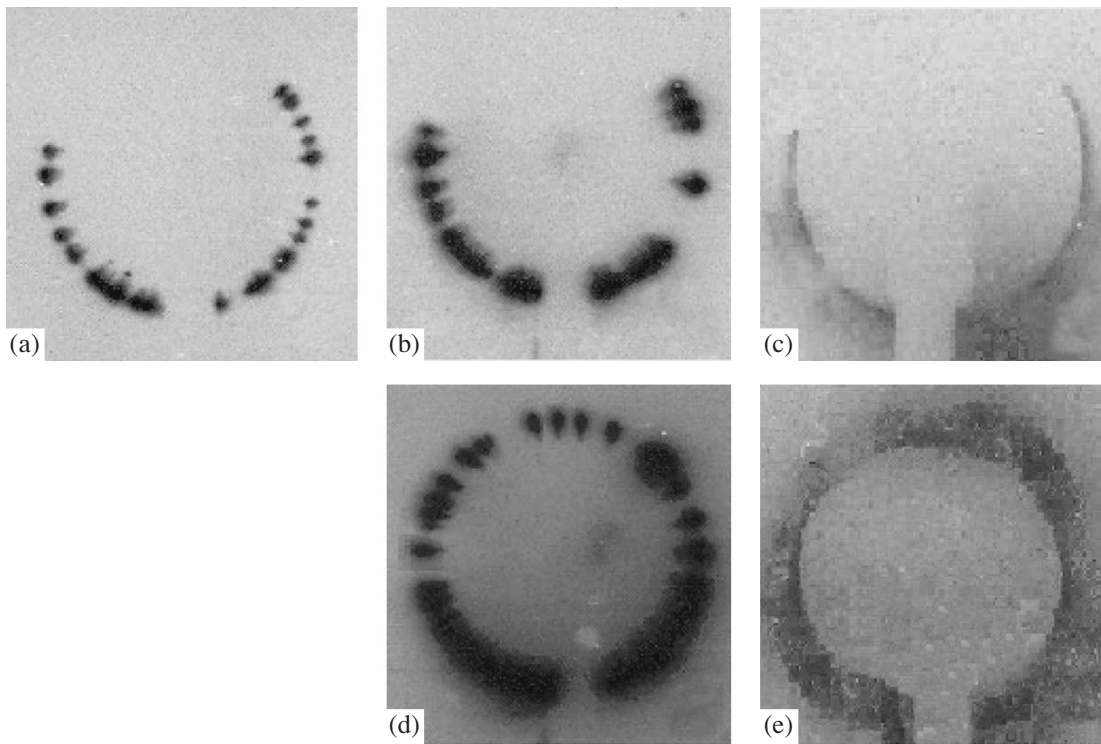


Fig. 11. Gap glow of the annular discharger: (a–c) photographs taken with an image tube with an exposure of 50 ns at different delay times t_{del} with respect to the gap breakdown, $t_{\text{del}} =$ (a) 0 and (b, c) 100 ns, and (d, e) integral photographs of the gap glow. The MG voltage is (a, b, d) 50 and (c, e) 110 kV.

sity released in this area (~ 0.1 J/cm), the time during which the gap parameters remain stable turns out to be fairly long (more than 1000 pulses).

Thus, the proposed electrode scheme of a millimeter vacuum gap substantially enhances its electric strength. In this case, the anode edge produces the twofold effect: (i) because of the concentration of the electric field at the edge, explosive emission begins at a higher gap voltage and (ii) the anode plasma produced by electron bombardment before the gap is bridged expands in the direction perpendicular to the anode surface (i.e., at an angle to the cathode); as a result, the gap is bridged more slowly, i.e., the pulse duration increases. The results of this study can be used in the Baikal project to develop and construct a multigap separating vacuum discharger for the matching of a multimodule POS to the liner load [1].

5. CONCLUSIONS

It is shown that the use of an intermediate inductance or a separating discharger to match a multimodule POS to the liner load, whose impedance is initially low and increases with time, eliminates the effect of the low-impedance load on the dynamics of the current break in the POS. In this case, the POS is decoupled from the low-impedance load by the high-

impedance matching element. This makes it possible to synchronize the POS modules and achieve efficient energy transfer to the liner. By properly choosing the parameters of the matching element (the value of the intermediate inductance or the value of the breakdown voltage of the separating discharger), one can control the output voltage, the amplitude and rise time of the load current, and the efficiency of energy transfer.

As a separating discharger, we propose to use a vacuum explosive-emission diode with a millimeter electrode gap. The anode has a sharp edge, and the cathode is planar. At a pulse duration of ~ 50 ns, the electric strength of such a gap can be as high as 1.8 MV/cm. In this case, a multichannel (~ 5 channel/cm) breakdown of the gap occurs, the breakdown time being ~ 10 ns.

A combined matching circuit consisting of an intermediate inductance and a separating discharger can also be used. The use of such a discharger lowers the requirements to both the POS–liner connection inductance and the electric strength of the separating discharger.

The above schemes for matching a multimodule POS to the liner load can be utilized in the Baikal project, intended to create a superpower pulsed generator for ICF experiments.

ACKNOWLEDGMENTS

This work was supported by the Committee on Atomic Science and Technology of the RF Ministry on Atomic Energy, the FR Program for State Support of Leading Scientific Schools (project no. NSh-5819.2006.2), and the Russian Foundation for Basic Research (project no. 06-02-08189).

REFERENCES

1. É. A. Azizov, S. G. Alikhanov, E. P. Velikhov, et al., *Vopr. At. Nauki Tekh., Ser. Termoyad. Sintez*, No. 3, 3 (2001).
2. N. U. Barinov, S. A. Budkov, G. I. Dolgachev, et al., *Fiz. Plazmy* **28**, 202 (2002) [*Plasma Phys. Rep.* **28**, 177 (2002)].
3. Yu. P. Golovanov, G. I. Dolgachev, L. P. Zakatov, et al., *Vopr. At. Nauki Tekh., Ser. Termoyad. Sintez*, No. 2, 35 (1987).
4. A. S. Chernenko, V. P. Smirnov, A. S. Kingsep, et al., in *Proceedings of the 14th IEEE International Pulsed Power Conference, Dallas, 2003*, Vol. 1, p. 167.
5. V. V. Aleksandrov, G. S. Volkov, E. V. Grabovski, et al., in *Proceedings of the 6th International Conference on Dense Z-pinches, Oxford, 2006*, AIP Conf. Proc. **808**, 3 (2006).
6. R. B. Spielman, F. Long, T. H. Martin, et al., in *Proceedings of the 10th IEEE International Pulsed Power Conference, Albuquerque, 2006*, Vol. 1, p. 396.
7. G. I. Dolgachev and A. G. Ushakov, *Fiz. Plazmy* **27**, 121 (2001) [*Plasma Phys. Rep.* **27**, 110 (2001)].
8. A. S. Altukhov, G. I. Dolgachev, D. D. Maslennikov, et al., *Fiz. Plazmy* **31**, 1104 (2005) [*Plasma Phys. Rep.* **31**, 1029 (2005)].
9. A. S. Altukhov, P. I. Blinov, G. I. Dolgachev, et al., *Fiz. Plazmy* **29**, 722 (2003) [*Plasma Phys. Rep.* **29**, 664 (2003)].
10. G. I. Dolgachev, D. D. Maslennikov, and A. G. Ushakov, *Prib. Tekh. Éksp.*, No. 5, 82 (2004).
11. G. A. Mesyats and D. I. Proskurovsky, *Pulsed Electrical Discharge in Vacuum* (Nauka, Novosibirsk, 1984; Springer-Verlag, Berlin, 1989).
12. G. I. Dolgachev and A. G. Ushakov, *IEEE Trans. Plasma Sci.* **35**, 110 (2007).
13. E. V. Grabovsky, E. A. Azizov, S. G. Alikhanov, et al., in *Proceedings of the 14th IEEE International Pulsed Power Conference, Dallas, 2003*, Vol. 2, p. 921.

Translated by N.F. Larionova

Copyright of Plasma Physics Reports is the property of Springer Science & Business Media B.V. and its content may not be copied or emailed to multiple sites or posted to a listserv without the copyright holder's express written permission. However, users may print, download, or email articles for individual use.